Semiconductor Physics, Quantum Electronics & Optoelectronics, 2006. V. 9, N 1. P. 36-42.

PACS 61.72.V; 72.80.E

Solid state doping of $Cd_xHg_{1-x}Te$ epitaxial layers with elements of V group

A.P. Vlasov[1], O.Yu. Bonchyk[2], I.M. Fodchuk[3], R.A. Zaplitnyy[3], A. Barcz[4], Z.T. Swiatek[5]
[1]I. Franko Lviv National University, 1, Universitetska str., 79000 Lviv, Ukraine
[2]Institute for Applied Problems of Mechanics and Mathematics, NAS of Ukraine
3-b, Naukova str., 79601 Lviv, Ukraine
[3]Yu. Fed'kovich Chernivtsi National University, 19, Universitetska str., 58012 Chernivtsi, Ukraine
[4]Institute of Physics of Polish Academy of Sciences, 32/46 Al. Lotnikow, 02-668 Warsaw, Poland
[5]Institute of Metallurgy and Materials Science, Polish Academy of Science
25 Reymonta Str., 30-059 Krakow, Poland

Abstract. Presented here are the results of studying the controlled doping with elements of V group of the periodic table, arsenic As and antimony Sb, of narrow gap $Cd_xHg_{1-x}Te$ epitaxial layers during the isothermal growth from the vapour phase by the evaporation-condensation-diffusion method. Three types of impurity sources have been used for solid state doping: homogeneously doped with As(Sb) single crystal substrates of CdTe, As doped buffer $Cd_yHg_{1-y}Te$ ($y > x$) epitaxial layers obtained by RF sputtering in mercury glow discharge onto undoped CdTe substrates, and As(Sb) implanted undoped CdTe substrates. The results of comparative analysis of galvano-magnetic measurements and SIMS spectra indicated very high, practically nearly ~100 %, electrical activity of dopants in the $Cd_xHg_{1-x}Te$ epitaxially grown layers.

Keywords: X-ray spectrometry, substrate, epitaxial layer.

Manuscript received 30.10.05; accepted for publication 15.12.05.

1. Introduction

The narrow-gap solid solutions of cadmium and mercury tellurides – $Cd_xHg_{1-x}Te$ ($x = 0.18…0.3$) are the most suitable semiconductor materials for producing high efficient detectors of infra-red radiation (IR) for 3 to 5 and 8 to 14 μm atmospheric windows [1]. In spite of the technological difficulties, high production cost and development of investigation of alternative materials, there exists the necessity to improve the methods of obtaining both $Cd_xHg_{1-x}Te$ itself and detectors based on it. When producing the photovoltaic detectors on the basis of $Cd_xHg_{1-x}Te$ epitaxial heterostructures, great efforts are being directed on obtaining a doped material with required electrophysical properties. The element of V group As is considered to be the most attractive acceptor impurity in $Cd_xHg_{1-x}Te$, since 100 % activation of acceptor states in the material may be reached at the concentration of $5\cdot10^{18}$ cm^{-3}. Nevertheless, such activation levels have been achieved at liquid-phase epitaxy from melts enriched with Hg. The doped epitaxial layers of $Cd_xHg_{1-x}Te$ obtained by molecular-beam epitaxy possess a *n*-type of conductivity after the growth, and to achieve high-level activation of the acceptor impurity, an additional annealing in Hg vapour is used [2]. Therefore, understanding of an amphoteric nature of the impurity and possibility to control the process of impurity incorporation in $Cd_xHg_{1-x}Te$ are necessary for obtaining the material suitable to produce high-quality photovoltaic structures.

The aim of this paper was to investigate the processes of autodoping with the acceptor impurity As (Sb) of $Cd_xHg_{1-x}Te$ epitaxial layers at isothermal vapour phase growth by the method of evaporation-condensation-diffusion (ECD).

2. Experimental techniques

During the EVC epitaxial growth of $Cd_xHg_{1-x}Te$ layers, we used the substrates with three types of impurity sources:

I. Homogeneously doped single crystals of CdTe grown by the Bridgmann method with impurity incorporated during the synthesis process at the concentration level of $N_{As}\sim10^{16}…10^{17}$cm^{-3} ($N_{Sb}\sim10^{17}…10^{18}$cm^{-3}).

II. Undoped CdTe (111) and CdTe (110) crystals on surfaces of which heavily doped with As ($N_{As}\sim10^{19}…10^{20}$ cm^{-3}) epitaxial buffer films of $Cd_yHg_{1-y}Te$ were deposited.

© 2006, V. Lashkaryov Institute of Semiconductor Physics, National Academy of Sciences of Ukraine

III. Undoped CdTe (111) and CdTe (110) crystals on surfaces of which controlled amount of As (Sb) was incorporated by ion implantation.

The surface sources of dopant of II type were produced by RF ($f = 13.56$ MHz) sputtering in mercury glow discharge of wider gap ($y > x$) $Cd_yHg_{1-y}Te$ epitaxial buffer films (y denotes the composition of a solid solution film with a dopant, whereas x denotes the composition at the surface of $Cd_xHg_{1-x}Te$ graded-gap epitaxial layers). To introduce As with concentrations greater than 1 at.%, the sputtering of the pure element along with the target material was carried out. For obtaining the concentration less than 0.01 at.% the impurity was introduced during the target synthesis using the weight of As. The contents of impurity in the film were controlled by the area from which the sputtering took place. When using the source of III type As(Sb) impurity was implanted with the equal ion energy $E = 100$ keV. Inhomogeneity of the dopant doze did not exceed 1 %, reproducibility was 98 %.

For implementation of the vapour-phase epitaxy [3], we used silica ampoules and accessory. Flatness and mirror-like surfaces of CdTe substrates were achieved by means of an abrasive-free chemico-mechanical polishing in a bromine-butanol etchant. The mounted ampoules were evacuated by oil-free pumping down to a residual pressure of $\sim 10^{-4}$ Pa, afterwards they were sealed and weighted in a two-zone furnace with resistive heating. In all experiments the temperature of growth zone amounted to 600 °C. The temperature of the other zone was maintained at the level that provided the pressure of the saturated mercury vapour during the epitaxial growth equal to $P_{Hg} = (2\ldots4)\cdot10^5$ Pa. In order to increase the number of mercury vacancies created at the final stage of $Cd_xHg_{1-x}Te$ epitaxy, an annealing in the isothermal regime in mercury vapour at the temperature 320 °C was carried out for 60 hours. At these regimes of growth and post-growth annealing undoped epitaxial layers of $Cd_xHg_{1-x}Te$ had n-type of conductivity.

Diagnostics of the structural changes in the near-surface regions of single crystals and epitaxial layers of $Cd_xHg_{1-x}Te$ was performed using the X-ray methods since they are non-destructive and highly sensitive to various types of distortions of atomic planes. For the research, the Berg-Barrett method in asymmetric and skew-symmetric geometry of backward diffraction was used [4, 5]. For obtaining the rocking curves (RC), we used the method of two-crystal spectrometer in a dispersionless scheme (n,–n). The skew-asymmetric scheme of X-ray diffraction makes it possible to investigate selectively and layer-by-layer with a step of ~0.05 µm and less the structural changes in the near-surface layers after the influence of different external factors, for example, ion implantation. By azimuth rotation of a crystal around the diffraction vector by the angle ψ, one can realize the case when the penetration depth of X-rays would be of the same order as the depth of the disturbed by ions near-surface layers

$$L_{ext} = \frac{\lambda}{|\chi_h|}\sqrt{\gamma_0|\gamma_h|}\,, \quad (1)$$

where

$$\gamma_{0,h} = -\cos\theta\cos\varphi\sin\psi \pm \sin\theta\cos\psi\,, \quad (2)$$

$$\gamma_{0,h} = \sin\phi_{0,h}\,, \quad (3)$$

where $\phi_{0,h}$ are the incidence and exit angles of X-rays, θ is the diffraction angle, ψ is the disorientation angle between the planes of incidence and reflection, L_{ext} is the extinction length, χ_h are the coefficients of Fourier-polarization, λ is the wavelength, the sign "plus" corresponds to the incident and "minus" – to the diffracted ray.

Table shows the galvanomagnetic properties of $Cd_xHg_{1-x}Te$ samples investigated by the standard technique of Hall measurements at $T = 77\ldots300$ K and the magnetic fields ranging from 0.005 to 1.7 T. The composition of $Cd_xHg_{1-x}Te$ epitaxial layers was controlled using the spectra of optical absorption.The distribution of impurity concentration and the profiles of composition of $Cd_xHg_{1-x}Te$ epitaxial layers were determined by the Secondary Ion Mass-Spectrography (SIMS) at Cameca IMS-6F device. Simultaneously the analysis of the impurity and the main component isotope of $Cd_xHg_{1-x}Te$ (^{202}Hg ^{130}Te or ^{202}Hg ^{133}Cs) has been carried out. The sensitivity limit of the device for the analyzed impurities was in the range from $5\cdot10^{14}$ to 10^{15} cm^{-3}.

The quantitative composition of the main components along the thickness of the grown epitaxial $Cd_xHg_{1-x}Te$ layer was determined from X-ray microanalysis spectra. Measurements of the spectra were performed on the sample cross cleavages by means of a Scanning Electron Microscope based on microanalyser JXA-50A (JEOL). The composition measurement error did not exceed 1%.

3. Results of researches

The $Cd_xHg_{1-x}Te$ epitaxial layers grown on the As homogeneously doped substrates of CdTe had the hole type of conductivity. The boundary of maximum penetration of Hg in the CdTe substrate is clearly seen in the SEM-microphotography of the cross cleavage of typical sample 73-2 grown on the CdTe substrate with $N_{As} \sim 10^{16}$ cm^{-3} (Fig. 1a). The composition-distribution curve measured with the help of X-ray microanalysis for the As doped epitaxial layer (Fig. 1a) does not differ from the typical composition profiles in $Cd_xHg_{1-x}Te$ samples obtained during the epitaxy on undoped CdTe substrates with the analogous growth regimes. Fig. 1a also shows the SIMS distribution along the depth of $Cd_xHg_{1-x}Te$ epitaxial layer. The acceptor concentration determined in this sample by means of galvanomagnetic

© 2006, V. Lashkaryov Institute of Semiconductor Physics, National Academy of Sciences of Ukraine

Table. Results of electrophysical investigation of doped with As (Sb) ECD epitaxial layers of $Cd_xHg_{1-x}Te$.

No	Sample number	Dopant source	x	d, μm	μ, cm²/(V·s)		R_H, cm³/Q		$N_a - N_d$, cm⁻³ 77 K
					273 K	77 K	273 K	77 K	
1	V-23	Undoped	0.23	64	7740	20050	–610	–1480	$4.2\cdot10^{15}$
As									
2	73-2	Substrate	0.213	57	3741	150	–293	+464	$1.35\cdot10^{16}$
3	770-V32	Buffer film	–	59	54	52	+16	+37	$1.7\cdot10^{17}$
4	771-V33	Buffer film	–	62	150	43	–91	+56	$1.12\cdot10^{17}$
5	77-2(110)	Implanted impurity	0.241	67	5850	329	–562	+518	$1.2\cdot10^{16}$
Sb									
6	80-5(Sb)	Substrate	0.19	70	10370	245	–200	+198	$3.17\cdot10^{16}$
7	80-6(Sb)	Substrate	0.24	80	11780	387	–268	+160	$3.3\cdot10^{16}$

measurements (Fig. 1b) corresponds to the real As concentration in the epitaxial layer and signifies the high (close to 100 %) level of the electrical activity of the impurity.

The successful use of the above described CdTe substrates for obtaining $Cd_xHg_{1-x}Te$ epitaxial layers incites the search of the alternative methods of the dopant source production. Figs 2a and 2b schematically show the structures with the impurity sources which are formed on the surface of undoped CdTe single crystals used as substrates for ECD epitaxy. Below, the results of the fulfilled investigation using such sources are presented.

When doping the $Cd_xHg_{1-x}Te$ ECD epitaxial layers by using the structures shown in Fig. 2a, the identical technological regimes for deposition of As highly doped films in samples 770 and 771 have been used. CdTe undoped single crystals with the (111) and (110) surface orientations were used.

The film thickness of the sample 770 was 6.5 μm and the estimated impurity concentration by the target doping level was estimated to be N_{As}~10^{19} cm^{-3}, and for the sample 771 – 5 μm and N_{As}~10^{20} cm^{-3}, correspondingly.

These heterostructures were applied for As doping of the $Cd_xHg_{1-x}Te$ ECD epitaxial layers – samples 770-V32 and 771-V33 (Table). The initial position of the impurity source in the buffer film is shown by rectangles on the corresponding SIMS plofiles (Fig. 3): the base corresponds to the film thickness, the height – to the impurity concentration in the target. After the completion of the epitaxy process in the sample 770-V32 (Fig. 3a), total smoothing of the As profile along the structure thickness has occurred, whereas in the sample 771-V33 (Fig. 3b) the source did not completely exhaust itself. The maximum residual concentration of As in the buffer film of the sample 771-V33 corresponds to the calculated concentration of dopants in the target. This is a confirmation of the effective incorporation of the impurity into $Cd_yHg_{1-y}Te$ films during the low temperature epitaxy in Hg glow discharge and, respectively, ensures the high efficiency of As doping for $Cd_xHg_{1-x}Te$ layers when used during ECD epitaxy [6].

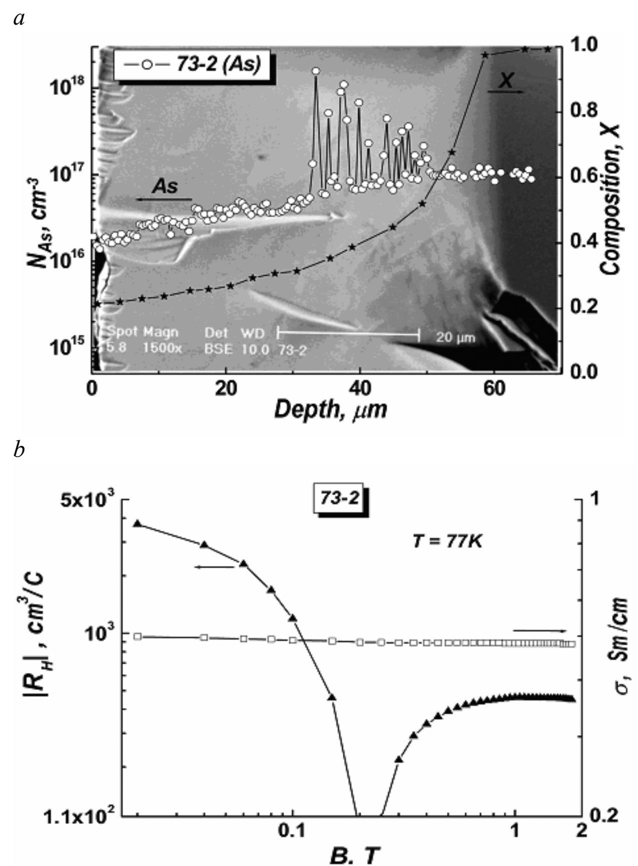

Fig. 1. a) SEM microphotography of the cross cleavage of sample 73-2 with the profile of composition distribution and SIMS distribution of As along the depth of $Cd_{0.21}Hg_{0.79}Te$ epitaxial layer; b) magnetofield dependences of the Hall coefficient and conductivity for the sample 73-2.

© 2006, V. Lashkaryov Institute of Semiconductor Physics, National Academy of Sciences of Ukraine

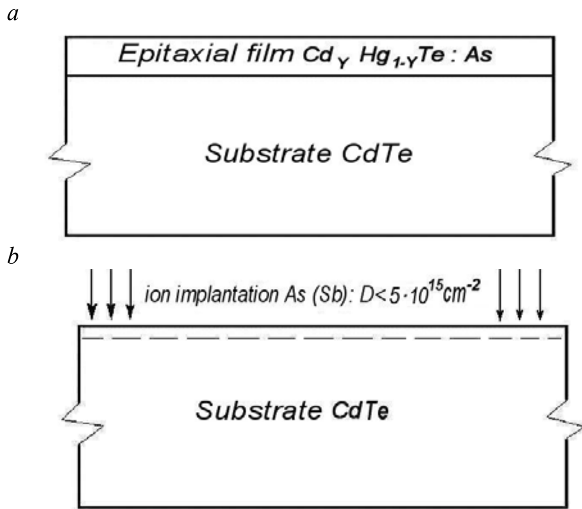

Fig. 2. Structure of substrates with surface impurity sources used at doping of $Cd_xHg_{1-x}Te$ epitaxial layers. Impurity source on CdTe undoped single crystal substrates: a) highly doped with the As wider gap ($y > x$) $Cd_yHg_{1-y}Te$ epitaxial film; b) surface layer of a substrate implanted with As (Sb) ions.

When using the As(Sb) ion implanted impurity source, the structures based on CdTe (Fig. 2b) were mounted immediately after the ion implantation without any additional chemical processing in silica ampoules and were loaded into furnaces for carrying out the ECD epitaxy process [7]. The grown layers had mirror-like surfaces.

At the initial stages of the epitaxial growth, the state of a substrate crystal structure is of paramount importance. For establishing the influence of the disturbed surface layer on the ECD epitaxy, we have carried out X-ray study of both CdTe substrates after ion implantation and $Cd_xHg_{1-x}Te$ doped epitaxial layers grown on them [8].

During the implantation of As ions, in the near surface regions of CdTe single crystal, the disorder and damages consisting of considerable concentration of intrinsic defects in two sublattices, cluster formations, as well as surface dislocations and stacking faults originate [9]. The set of these imperfections causes the creation of strained regions in the surface layers of a crystal, which is correspondingly reflected in the X-ray topograms and swing curves. Fig. 4 shows the most typical topograms of the CdTe single crystal surface obtained in the asymmetric (Fig. 4a) and skew-asymmetric (Fig. 4b) diffraction schemes. A peculiarity of the studied sample lies in the fact that in CdTe substrate prepared by the standard procedure As ions are implanted only into the half of its surface. In the implanted part (A) of the crystal, in contrast to the non-implanted one (B), there takes place a distortion and tailing (331) of the reflexes of the $CuK_{\alpha1,2}$ line doublet. The reason for this is both the bulk disturbances of crystal perfection – the availability of the fragment structure or low-angle boundaries (Fig. 4a) and the gradient of the lattice parameter in certain crystallographic directions on the crystal surface. At azimuth rotation of a crystal around the diffraction vector, the tailings and mergings of the diffraction maxima are observed in the topograms. During the penetration of X-rays at the depth $L_{ext} \sim 0.35$ μm, the part of the crystal no longer diffracts X-rays (Fig. 4b). Such a picture is caused by the great disorder of the crystal lattice in the subsurface layers at the depth up to 0.35 μm and gives rise to the strains at the interface between surface layer and implant on one side and CdTe crystal on the other.

The swing curves obtained from the As implanted crystal parts (Fig. 5a) are characterized by an increase in the curve shape asymmetry and the magnitudes of its half-width (approximately by 2 to 2.5 times). The small decay in amplitude oscillations is observed near the main maximum of the intensity. This is mainly caused by the presence of the gradient of lattice distance along the crystal normal in the implanted region. Such gradient changes in the lattice parameter amount up to $1.1\cdot10^{-4}\ldots2.3\cdot10^{-4}$ Å.

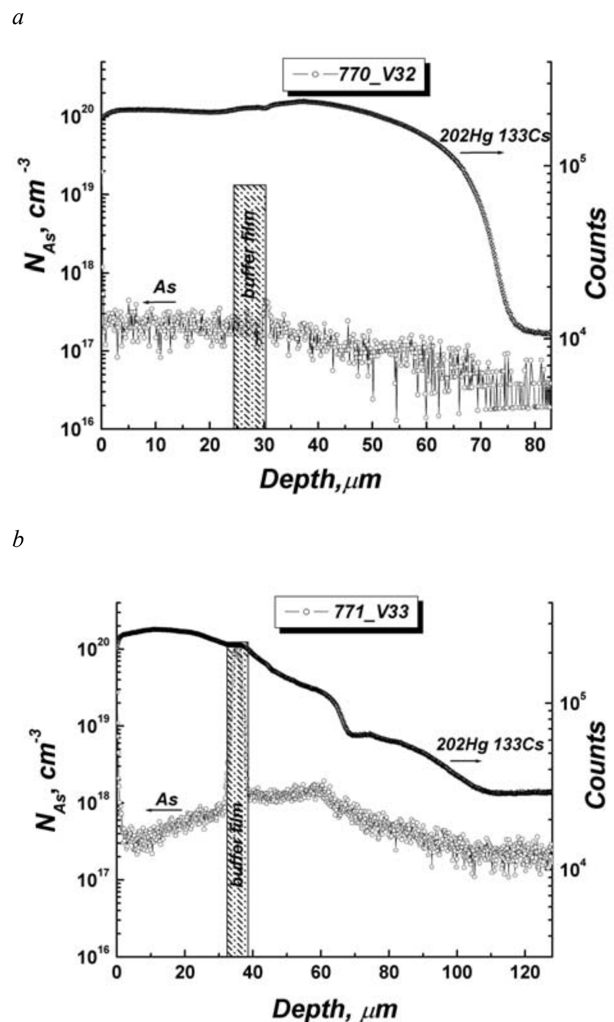

Fig. 3. SIMS distribution of the As concentration and $^{202}Hg^{133}Cs$ signal along the thickness of $Cd_xHg_{1-x}Te$ ECD epitaxial layers grown on undoped epitaxial buffer films of $Cd_yHg_{1-y}Te$. For the sample 770-V32: $N_{As} \sim 10^{19}$ cm^{-3}, CdTe (111) (a), 771-V33: $N_{As} \sim 10^{20}$ cm^{-3}, CdTe (110) (b).

© 2006, V. Lashkaryov Institute of Semiconductor Physics, National Academy of Sciences of Ukraine

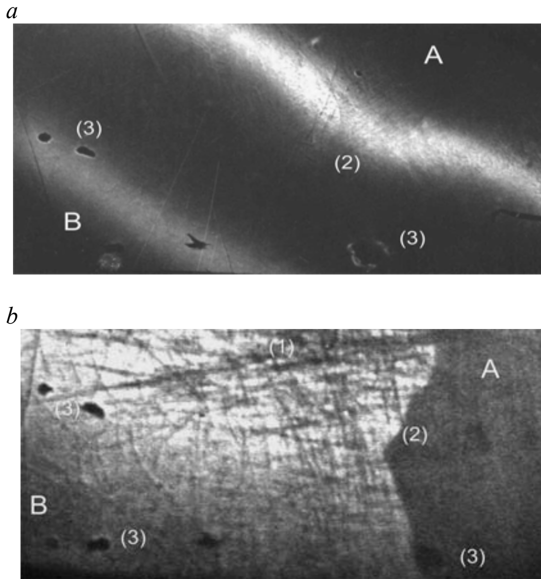

Fig. 4. X-ray topogram of CdTe single crystal. CuK_α-radiation, (111) surface of incidence: asymmetric scheme of diffraction, (331) reflection, ×18, $L_{ext} = 2.6$ µm (a), skew-asymmetric scheme, (511) reflection, ×18, $L_{ext} = 0.35$ µm (b). Mechanical damages – (1), interface between doped and undoped regions – (2), inclusions (minimal size – 60-90 µm, maximal size – 300 µm) – (3).

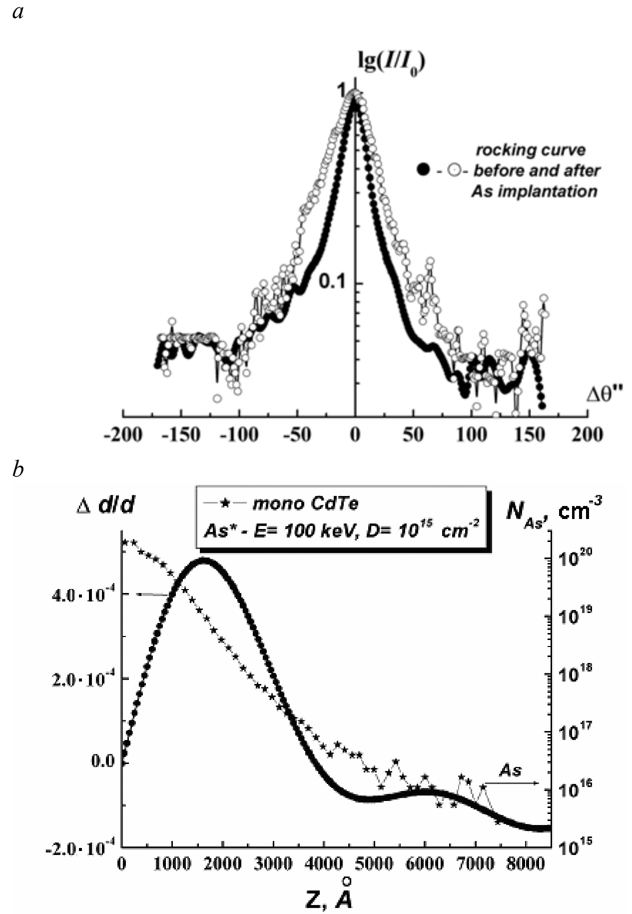

Fig. 5. Rocking curves of diffraction reflection of CdTe single crystal. CuK_α-radiation, symmetric scheme of diffraction, (111) incidence, (333) reflection (a). Profiles of deformation and impurity distribution in the near surface region of CdTe (111) crystal after As implantation (b).

Using the numerical method of RC modeling based on semikinematic approximation of the X-ray scattering, the thickness of the disturbed layer on CdTe surface after As ion implantation ($E = 100$ keV; $D = 1\cdot10^{15}$ cm^{-2}) has been determined [8, 9]. The region of the large disorder lies in the range of ~0.3…0.35 µm and the total region of marked structural disturbance extends to the depth of ~0.6…0.8 µm from the surface.

To determine the depth distribution of strains in the near surface layer, we have used approaches based of the basic principles of the dynamic theory of the X-ray scattering – numerical solutions of the Takagi differential equation system and comparison of the obtained results with the experimental data [10]. The calculated profile of deformation and corresponding SIMS profile of the impurity distribution in the near surface region of CdTe single crystal after As implantation are demonstrated in Fig. 5b.

The $Cd_{0.24}Hg_{0.76}Te$ epitaxial layer of the sample 77-2 (Table) was grown on CdTe (110) substrate in which As ions with the dose $D = 10^{15}$ cm^{-2} had been implanted. The characteristic form of the thickness dependence of the impurity concentration in the grown layer in the sample 77-2 (Fig. 6a) is slightly different for the epitaxial layers grown on the implanted surface of CdTe (111) undoped substrates. Fig. 6b shows the magnetofield dependences of the Hall coefficient and conductivity of this sample at $T = 77$ K, which indicates the high level of electrical activity of the impurity in the obtained epitaxial layer.

It follows from the analysis of X-ray structural data (Fig. 7) that the grown layers are perfect – in the topograms (Fig. 7a) a clear separation of the K_α-doublet lines is seen. At the same time, there are local regions that do not diffract X-rays, with a density of $\approx 10^3$ cm^{-2} and dimensions of 50–100 µm, among them tellurium inclusions are possible. The RC intensity distribution shown in Fig. 7b has a characteristic Gaussian form. The half-width of the rocking curves for the sample 77-2 is in the range of 70'' to 80''. This is indicative of the fact that annihilation of radiation defects and recrystallization of the disordered near surface layers in CdTe substrate occur at the initial stages of ECD epitaxy and do not result in deterioration of the crystal structure in $Cd_xHg_{1-x}Te$ doped epitaxial layers.

The high efficiency of doping from the As solid state source during the ECD epitaxial growth [7] has given an incitement to use another element of V group, Sb, as an impurity. Its successful usage for the liquid phase epitaxial layers of $Cd_{0.22}Hg_{0.78}Te$ has been shown by the

© 2006, V. Lashkaryov Institute of Semiconductor Physics, National Academy of Sciences of Ukraine

authors of the paper [13]. The choice of antimony is caused by the following reason. Impurities of V group (P, As) in CdTe crystals are shallow acceptors [14]. This provides comparatively high conductivity of this material, and Sb doping provides the possibility of obtaining semiisolating material where the conductivity is controlled by deep acceptors with energy separated levels [15]. The latter is attractive from the viewpoint of improving the electrophysical properties of $Cd_xHg_{1-x}Te$ epitaxial layers. This takes place due to the reduction of the influence of transition regions epitaxial layer – substrate on these properties.

We used the homogeneously Sb doped CdTe single crystals ($N_{Sb} \sim 10^{17}$ cm^{-3}) and the structures shown in Fig. 2b as substrates for epitaxial growth of $Cd_xHg_{1-x}Te$ by the ECD method. Table lists the resulting electrophysical properties of the $Cd_xHg_{1-x}Te$ ECD epitaxial layers of samples 80-5 and 80-6. In both cases, we can observe that, during the epitaxy, similarly to As doping, there occurs uniform doping of the grown graded-gap layer of $Cd_xHg_{1-x}Te$ with Sb, and the carrier concentration correlates with the Sb concentration determined by the SIMS technique.

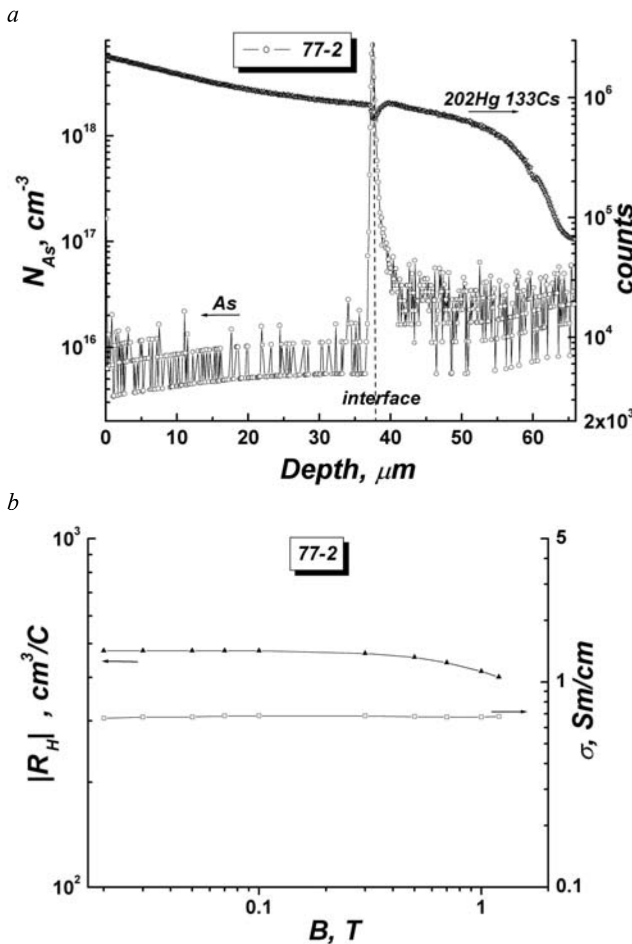

Fig. 6. SIMS distribution of As and $^{202}Hg^{133}Cs$ signal along the thickness of $Cd_xHg_{1-x}Te$ ECD epitaxial layer of the sample 77-2 (a); magnetofield dependences of the Hall coefficient and conductivity (b).

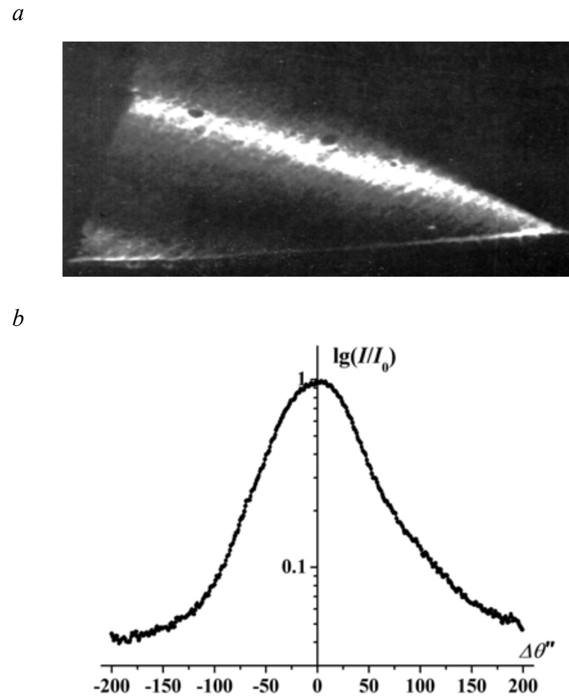

Fig. 7. Topogram of the sample 77-2. CuK_α-radiation, (111) surface of incidence: symmetric scheme of diffraction, (333) reflection, ×18, L_{ext} = 7.6 μm (a); rocking curve of the sample 77-2 (b).

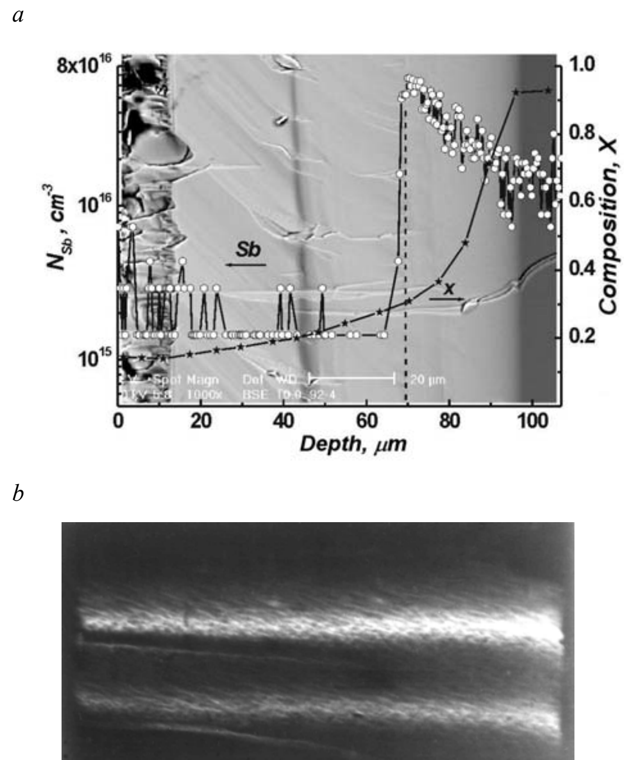

Fig. 8. SEM microphotograph of cross cleavage of the sample 92-4 with the profile of composition distribution and SIMS distribution of Sb along the thickness of $Cd_xHg_{1-x}Te$ epitaxial layer (a); topogram of the sample 92-4: CuK_α-radiation, skew-asymmetric scheme of diffraction: (111) plane of incidence, (511) reflection – φ = 90°, Φ_0=29°, L_{ext} = 1.01 μm (b).

© 2006, V. Lashkaryov Institute of Semiconductor Physics, National Academy of Sciences of Ukraine

For example, Fig. 8a illustrates the typical SEM microphotography of the cross cleavage with the shown distribution profiles of both the impurity and composition measured using the X-ray microanalyser for the sample 92-4, where the implanted with Sb undoped CdTe surface was used as a dopant source ($E = 100$ keV, $D = 8\cdot10^{14}$ cm^{-2}).

For the study of quality of the grown epitaxial layers, we have carried out X-ray topographical investigation. Fig. 8b shows the topogram of the sample 92-4 where the lines of K_α-series are separated without broadening and distortion. This allows one to conclude that grown $Cd_xHg_{1-x}Te$ epitaxial layers doped with Sb are uniform and structurally perfect.

4. Conclusions

$Cd_xHg_{1-x}Te$ epitaxial layers with close to 100 % level of electrical activity of the impurities have been obtained using doping with arsenic (antimony) during isothermal vapour phase epitaxy.

Investigation of the peculiarities of ion implantation of the epitaxial layers allows to obtain information concerning the behaviour of physical processes and establish the mechanisms responsible for changes in the defect sub-system of $Cd_xHg_{1-x}Te$ epitaxial layers.

The structural defects in disordered regions of radiation damages, which are created during the As (Sb) implantation with an energy of 100 keV in the near surface layers of CdTe single crystal substrates at irradiation doses of $D < 5\cdot10^{15}$ cm^{-2}, annihilate at the initial stages of epitaxy and virtually do not influence the structural perfection of the grown $Cd_xHg_{1-x}Te$ epitaxial layers.

References

1. A. Rogalski, Mercury cadmium telluride photodiodes at the beginning of the next millennium // *Defence Science Journal* **51**(1), p. 5-34 (2001).
2. S. Sivananthan, P.S. Wijewarnasuriya, F. Aqariden, H.R. Vydyanath, M. Zandian, D.D. Edwall, J.M. Arias, Mode of arsenic incorporation in HgCdTe grown by MBE // *J. Electron. Mater.* **26**, No 6, p. 621-624 (1997).
3. V.G. Savitsky, O.P. Storchun, Preparation of $Hg_{1-x}Cd_xTe$ ($0.1 \le x \le 0.5$) epitaxial layers by two-stage evaporation-condensation-diffusion method // *Thin Solid Films* **317**, p. 105-107 (1998).
4. S.A. Stepanov, E.A. Kondrashkina, A.N. Chuzo, An improved method of intergal characteristics for X-ray analysis of surface layers of crystals // *Poverkhnost'. Fizika, khimiya, mekhanika* No 9, p. 112-118 (1988) (in Russian).
5. V.G. Kon, M.V. Prilepskii, I.M. Sukhodreva // *Ibid.* No 4, p. 122(1984) (in Russian).
6. L.G. Mansurov, A.P. Vlasov, O.P. Storchun, B.O. Simkiv, V.K. Pysarevskii, I.M. Fodchuk, Managed conditions in epitaxial growth of HgCdTe by evaporation-condensation-diffusion method and their quality control // *Collected Scientific Papers of G.V. Karpenko Physico-Mechanical Institute of Academy of Sciences of Ukraine. Issue 9: Physical methods and means of monitoring of environment, materials and products.* Kyiv (2002) p.250-254.
7. A. Vlasov, V. Pysarevsky, O. Storchun, A. Shevchenko, A. Bonchyk, H. Pokhmurska, A. Barcz, Z. Swiatek, Controlled arsenic diffusion in epitaxial $Cd_xHg_{1-x}Te$ layers in the evaporation-condensation-diffusion process // *Thin Solid Films* **403-404**, p. 144-147 (2002).
8. A. Vlasov, A. Bonchyk, I. Fodchuk, P. Zaplitnyi, X-ray methods of X-ray analysis of CdHgTe epitaxial layers // *Collected Scientific Papers of G.V. Karpenko Physico-Mechanical Institute of Academy of Sciences of Ukraine. Issue 9: Physical methods and means of monitoring of environment, materials and products.* Kyiv (2004) p. 156-159.
9. M.H. Aguirre, H.R. Canepa, Ar-implanted epitaxially grown HgCdTe: evaluation of structural damage by RBS and TEM // *Nucl. Instr. and Meth. Phys. Res.* **B 175-177**, p. 274-279 (2001).
10. P.H. Kyutt, Three crystal X-ray diffractometry of superlattices and other multilayer epitaxial structures // *Metallofizika i novejshyie tekhnologii* **24**(4), p. 497-512 (2002) (in Russian).
11. D.K. Boun, B.K. Tanner, *High resolution X-ray diffractometry and topography*. Nauka, St.-Petersburg, 2002 (in Russian).
12. A.M. Afanas'ev, S.S. Fanchenko, On the reconstruction of profiles of disturbances in the near surface layers using X-ray diffraction data // *Krystallografiya* **287**(6), p. 1395-1399 (1986) (in Russian).
13. M.C. Chen, I.A. Dodge, Electrical properties of antimony doped p-type $Hg_{0.78}Cd_{0.22}Te$ liquid-phase epitaxy films // *Solid State Communs* **59**, No 7, p. 449-452 (1986).
14. E. Molva, Le Si Dang, Magneto-optical studies of excitons bound to Ag and Cu in p-type CdTe // *Phys. Rev. B* **127**, No 10, p. 6222-6226 (1983).
15. Y. Iwamura, S. Yamamori, H. Negishi, M. Moriyama, Deep levels of high resistivity Sb doped CdTe // *Jpn J. Appl. Phys.* **124**, No 3, p. 361-362 (1985).

© 2006, V. Lashkaryov Institute of Semiconductor Physics, National Academy of Sciences of Ukraine